

Effect of Schiff bases containing pyridyl group as corrosion inhibitors for low carbon steel in 0.1 M HCl

A. YURT^{1,*}, G. BERKET¹, A. KIVRAK¹, A. BALABAN² and B. ERK²

¹Faculty of Arts and Science, Chemistry Department, Osmangazi University, Eskisehir, Turkey

²Faculty of Science, Chemistry Department, Gazi University, Ankara, Turkey

(*author for correspondence, tel.: +90-222-2290433; fax: +90-222-2393578; e-mail: ayurt@ogu.edu.tr)

Received 5 December 2004; accepted in revised form 3 May 2005

Key words: corrosion, hydrochloric acid, inhibitor, low carbon steel, Schiff bases

Abstract

The inhibiting effect of four newly synthesised Schiff bases containing pyridyl group was investigated on the corrosion of low carbon steel in 0.1 M hydrochloric acid solution under various conditions by potentiodynamic polarisation method and impedance measurements. The Schiff bases used were 2-((1Z)-1-aza-2-(2-pyridyl)vinyl)benzene-1-thiol, (1Z)-1-aza-1,2-di(2-pyridyl)ethene, [((1Z)-1-aza-2-(2-pyridyl)vinyl)amino]benzene-1-thione and 2-((1Z)-1-aza-2-(2-pyridyl)vinyl)benzothiazole. All the Schiff bases inhibit corrosion of low carbon steel and their inhibition efficiencies increase with decrease in temperature and increase in concentration. The difference in protection actions of the inhibitors can be attributed to the presence of substituents in the structures that increase or decrease the electron density on the azomethine ($-C=N-$) group. Polarisation curves indicate that the Schiff bases act as anodic inhibitors. AC impedance and potentiodynamic polarisation measurements reveal that the compounds are adsorbed on the steel surface and the adsorption obeys the Temkin isotherm. Activation parameters (E_a , ΔH^* , ΔS^*) for the corrosion of low carbon steel in 0.1 M HCl were calculated and showed that corrosion was much reduced in the presence of inhibitors.

1. Introduction

Heterocyclic compounds such as Schiff bases are widely used in diverse industries for preventing corrosion of mild steel, aluminium alloys and copper in acidic media [1–3]. The action of such inhibitors depends on the specific interaction between the functional groups and the metal surface. Heteroatoms such as nitrogen, oxygen and sulphur play a crucial role owing to their free electron pairs [4]. Compounds with π -bonds also exhibit good inhibiting properties due to the interaction of the π electrons with the metal surface. Because Schiff bases have the general formula of $RC=NR'$, the above mentioned features combined with their structures suggest that such compounds should be good corrosion inhibitors.

Some Schiff bases have recently been reported as effective corrosion inhibitors for mild steel [5, 6], aluminium alloys [7] in acidic media and for halide corrosion of copper [8, 9].

In this study, the inhibiting effects of four Schiff bases having heteroaromatic compounds of nitrogen and/or sulphur as substituents, have been investigated for the corrosion inhibition of low carbon steel in 0.1 M HCl solution. The effects of concentration, temperature and

substituents on the inhibition efficiencies have been studied.

2. Experimental procedure

The working electrode was prepared from a cylindrical carbon steel bar (0.4% C, 0.9% Mn, 0.04% P, 0.04% S, 98.62% Fe). The electrode was sealed in a Teflon tube with polyester leaving only the working area exposed. The exposed surface (0.3526 cm²) was polished using different grades of emery paper (600, 800 and 1200) prior to each experiment, and then rinsed with triple distilled water and finally degreased with acetone.

The formulae of the investigated Schiff bases, synthesised according to the published methods [10–13], are shown in Figure 1. Solutions were prepared using triple distilled water and deaerated by bubbling ultra pure oxygen-free nitrogen gas for 60 min before use and this was continued during the measurements.

The measurements were performed in a three-compartment electrochemical cell with a separate compartment for the reference electrode connected with the main compartment via a Luggin capillary. The reference electrode was a silver–silver chloride ($Ag|AgCl|Cl^-$)

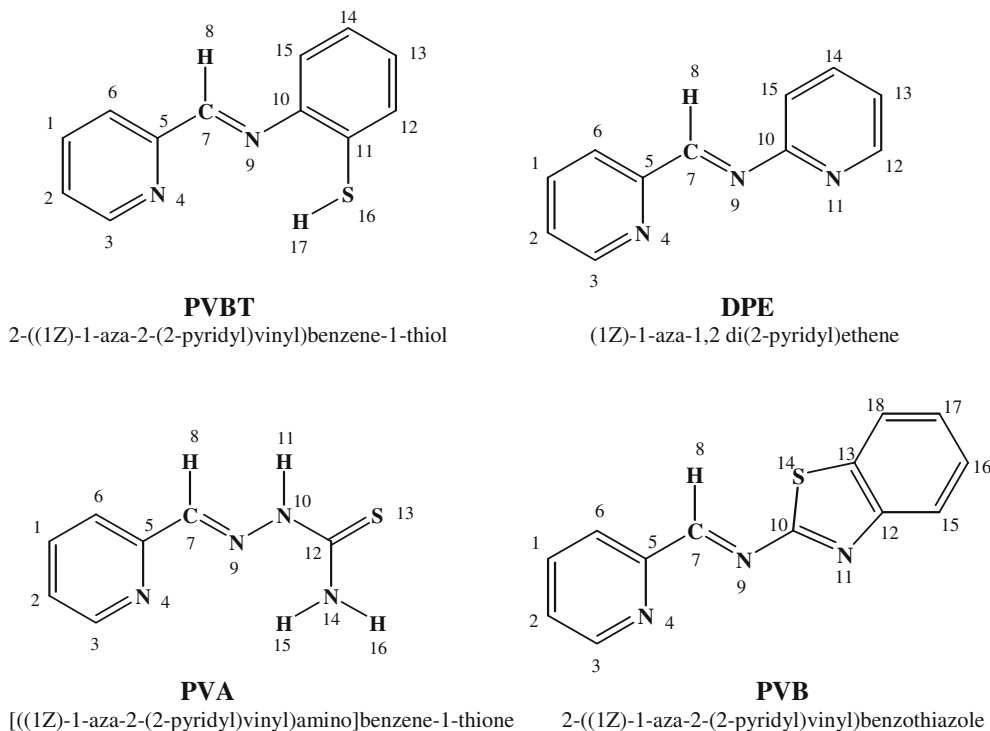


Fig. 1. Molecular structures of the investigated Schiff bases.

electrode and the auxiliary electrode was platinum. The cell was water-jacketed and connected to a Giant LTD6-G model Thermostat. Potentiodynamic polarisation and electrochemical impedance spectroscopy (EIS) measurements were performed using a CHI 604 Electrochemical Analyser. The working electrode was first immersed in the test solution for 60 min to establish a steady state open-circuit potential. After measuring the open-circuit potential, potentiodynamic polarisation curves were obtained at a scan rate of 0.5 mV s^{-1} in the potential range -600 to $+600 \text{ mV}$ relative to the corrosion potential. Corrosion current density values were obtained using Tafel extrapolation.

EIS measurements were performed at the open-circuit potential in the frequency range 100 kHz – 1 Hz with a signal amplitude perturbation of 5 mV in 0.1 M HCl at $20 \text{ }^\circ\text{C}$. All experiments were performed using a three-electrode system.

3. Results and discussion

3.1. Potentiodynamic polarisation and EIS results

Figure 2 shows the anodic and cathodic polarisation curve of low carbon steel in 0.1 M HCl solution in the absence and presence of DPE. Similar polarisation curves were obtained in 0.1 M HCl solutions with different concentrations of PVBT, PVA and PVB. Electrochemical parameters obtained from the Tafel extrapolation of the polarisation curves are given in Table 1. Both the cathodic and anodic curves show a

lower current density in the presence of the DPE, PVBT, PVA and PVB additives than those recorded in HCl solution and increase in the concentrations of the Schiff bases causes shifts of the corrosion potentials in the noble direction and variation in both Tafel slopes. Since the corrosion potential increases and corrosion rate decreases in the presence of inhibitors, the compounds studied are anodic inhibitors [14].

The influence of temperature on the inhibition properties of the Schiff bases was also studied by potentiodynamic polarisation. Typical polarisation curves obtained at 20 , 30 , 40 and $60 \text{ }^\circ\text{C}$ in the presence of $5 \times 10^{-4} \text{ M DPE}$ are shown in Figure 3. Similar temperature dependence

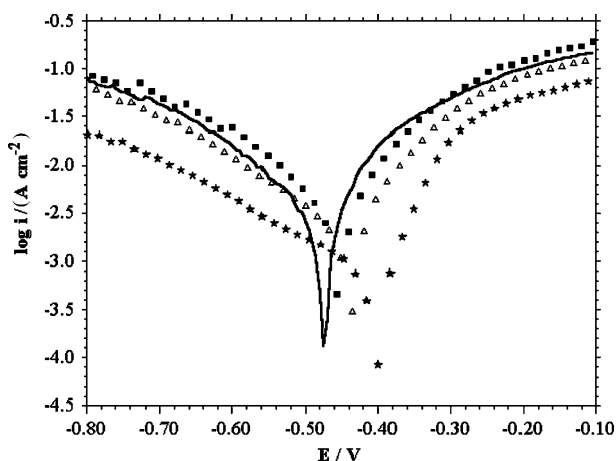


Fig. 2. Tafel polarization curves for low carbon steel in 0.1 M HCl solution in the absence (—) and presence of $5 \times 10^{-4} \text{ M}$ (★), $5 \times 10^{-5} \text{ M}$ (△) and $5 \times 10^{-6} \text{ M}$ (■) DPE.

Table 1. Tafel polarisation parameters, electrochemical parameters of impedance and corresponding inhibition efficiencies for the corrosion of low carbon steel in 0.1 M HCl without and with addition of various concentrations of investigated Schiff bases at 20 °C

Inhibitor	Concentration /M	E_{corr} /mV	i_{corr} / $\mu\text{A cm}^{-2}$	β_a /mV	β_c /mV	%IE	θ	R_s / Ω	R_t / Ω	%IE
–	0.1	–481	1380	141	–197	–	–	12.00	41	–
PVBT	5×10^{-6}	–443	870	92	–187	36.9	0.369	8.47	49	16
	1×10^{-5}	–440	537	75	–181	61.0	0.610	7.36	52	21
	5×10^{-5}	–426	186	74	–165	86.5	0.865	13.75	58	29
	1×10^{-4}	–454	74	86	–172	94.6	0.946	12.77	69	41
DPE	5×10^{-4}	–452	30	83	–127	97.8	0.978	10.73	102	58
	5×10^{-6}	–472	1258	148	–159	14.9	0.149	10.22	48	14
	1×10^{-5}	–466	891	132	–166	33.0	0.330	12.70	53	22
	5×10^{-5}	–450	794	123	–202	42.4	0.424	11.96	62	33
PVA	1×10^{-4}	–436	758	100	–223	45.0	0.450	12.13	68	39
	5×10^{-4}	–403	544	59	–223	60.5	0.605	12.97	88	53
	5×10^{-6}	–468	1282	134	–180	7.1	0.071	9.70	44	6
	1×10^{-5}	–449	1196	114	–178	13.3	0.133	10.45	48	14
PVB	5×10^{-5}	–434	912	104	–244	33.9	0.339	10.65	52	21
	1×10^{-4}	–430	851	99	–242	38.3	0.383	10.72	66	37
	5×10^{-4}	–406	549	96	–292	60.2	0.602	10.21	83	50
	5×10^{-6}	–455	1258	122	–167	8.8	0.088	13.63	42	2.3
PVB	1×10^{-5}	–451	1071	114	–173	22.4	0.224	14.23	46	11
	5×10^{-5}	–436	1018	94	–186	26.2	0.262	11.58	50	18
	1×10^{-4}	–437	914	90	–190	33.7	0.337	14.83	52	21
	5×10^{-4}	–408	660	87	–217	52.1	0.521	12.02	60	31

polarisation curves were also produced in the presence of 5×10^{-4} M PVBT, PVA and PVB and corrosion characteristics obtained from the Tafel polarisation curves are given in Table 2. The inhibiting efficiency increases with decrease in temperature and the corrosion potential values, given in Table 2, show that all compounds behave as anodic inhibitors at all temperatures.

The corrosion inhibition behaviour of low carbon steel in 0.1 M HCl with different concentrations of the Schiff bases was investigated by EIS. Figure 4 shows the impedance diagrams for low carbon steel in 0.1 M HCl solution in the absence and presence of various concentrations of DPE. Similar Nyquist diagrams and their corresponding Bode plots were also obtained in 0.1 M HCl with PVBT, PVA and PVB. The Nyquist diagrams

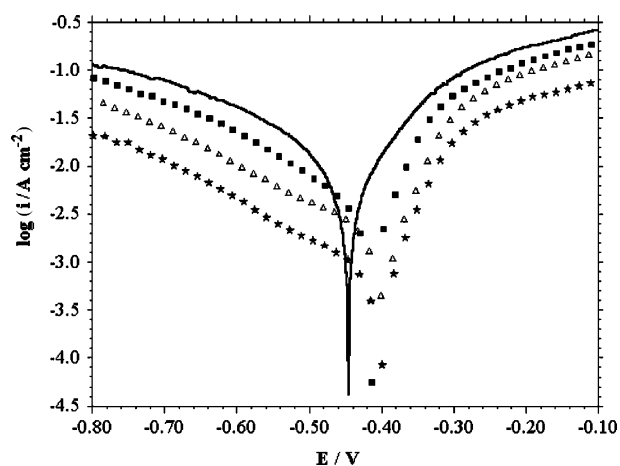


Fig. 3. Tafel polarisation curves for low carbon steel in 0.1 M HCl solution in the presence of 5×10^{-4} M DPE at 20 °C (★), 30 °C (△), 40 °C (■) and 60 °C (—).

present semi-circles and the Bode plots display a linear relation between $\log Z$ and $\log \text{freq}$. Fitted curves are plotted in terms of the equivalent circuit depicted in Figure 5 with the elements of the equivalent circuit (Table 1) [15].

In general the impedance loops measured are often depressed semi-circles with their centre below the real axis. This kind of phenomenon is known as the dispersing effect [16, 17]. But in this study, the complex impedance plots have the appearance of one capacitive contribution represented by one regular semi-circle for all solutions. A characteristic feature of the results was the absence of a diffusive contribution to the real impedance (Z') at low frequencies. This indicates that adsorbed Schiff bases inhibited anodic dissolution of metal effectively and the corrosion behaviour was charge transfer controlled [18].

Solution resistance, R_s , and charge transfer resistance, R_t , values were obtained from Nyquist plots. Inhibition efficiencies, IE, were calculated using the following formula (Equation 1)

$$\%IE = [(R_t - R_{t0})R_t] \times 100 \quad (1)$$

where R_t and R_{t0} are values of the charge transfer resistance in the presence and absence of inhibitor, respectively.

From Figure 4, comparing the impedance behaviour of low carbon steel in HCl solution in the presence and absence of a Schiff base, the corrosion of low carbon steel is obviously inhibited in the presence of additive. The quantitative results can be seen in Table 1; the inhibiting efficiencies of the four inhibitors increase with increasing concentration. This behaviour reveals that the Schiff bases are adsorbed on the steel.

3.2. Factors influencing the inhibition efficiency

It is evident from Tables 1 and 2 that all the Schiff bases are effective corrosion inhibitors in 0.1 M HCl. Increase in inhibition efficiencies with increase in concentration indicates that inhibition is due to adsorption on the steel surface.

It is generally assumed that the adsorption of inhibitor at the metal/solution interface is the first step in the

mechanism of inhibition in acidic media. Four types of adsorption may take place by organic molecules at the metal/solution interface: (1) Electrostatic attraction between the charged molecules and charged metal; (2) Interaction of uncharged electron pairs in the molecule with the metal; (3) Interaction of π electrons with the metal and (4) Combination of 1 and 3. Chemisorption involves the sharing or transfer of charge from the molecules to the surface to form a coordinate type bond.

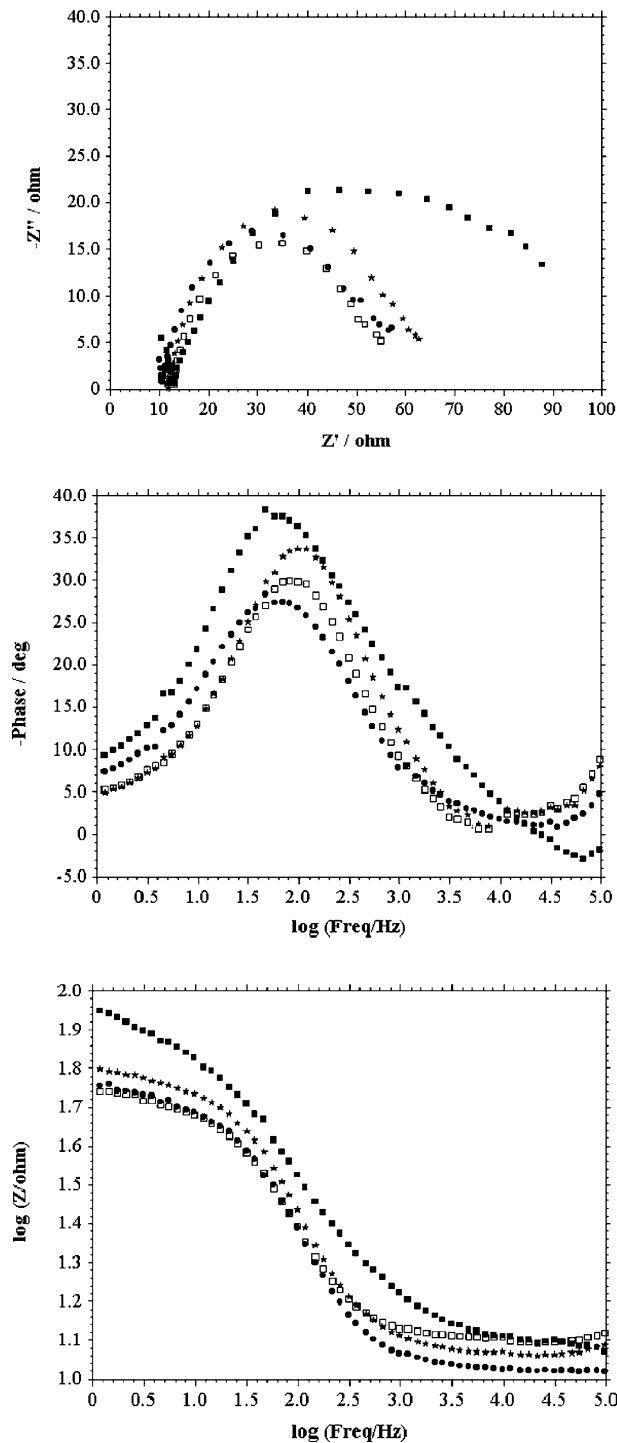


Fig. 4. Nyquist plots and Bode plots for low carbon steel in 0.1 M HCl solution in the absence (\square) and presence of 5×10^{-4} M (\blacksquare), 5×10^{-5} M (\blackstar) and 5×10^{-6} M (\bullet) DPE.

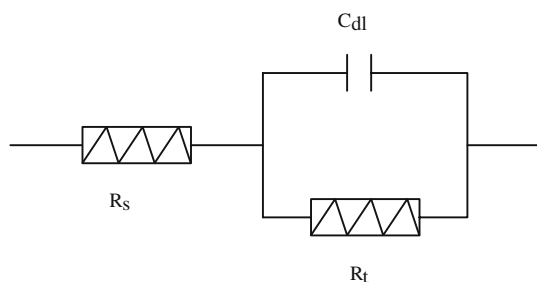


Fig. 5. Electrochemical equivalent circuit diagram for metal–electrolyte interface.

Electron transfer is typical for transition metals having vacant low-energy orbitals. As for inhibitors, electron transfer can be expected with compounds having relatively loosely bound electrons [19].

The establishment of isotherms that describe the adsorption behaviour of corrosion inhibitor is important as they can provide important clues about the nature of metal–inhibitor interaction. Determination of the type of adsorption isotherm, taking into account the degree of surface coverage, θ , as a function of inhibitor

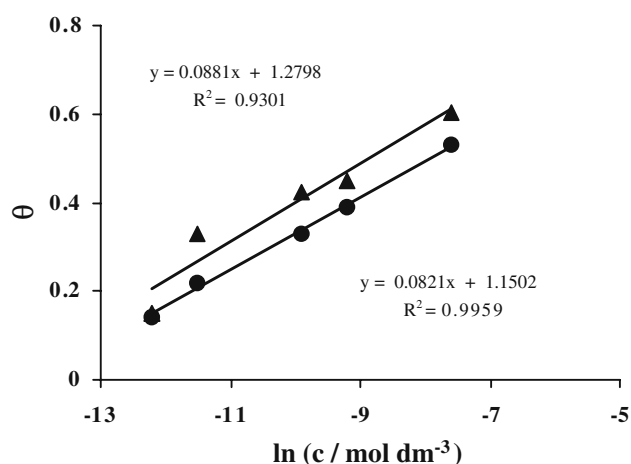


Fig. 6. Plot of Temkin adsorption isotherm of DPE obtained by using surface coverage values calculated by the EIS (●) and Tafel polarisation (▲) results.

concentration. The surface coverage values were calculated from Equation 2:

$$\theta = [1 - (i_{\text{inh}}/i_{\text{uninh}})] \quad (2)$$

Table 2. Tafel polarisation parameter values and corresponding inhibition efficiencies for the corrosion of low carbon steel in 0.1 M HCl without and with addition of 1×10^{-5} and 5×10^{-4} M concentrations of Schiff bases at different temperatures

Inhibitor	Temperature /°C	Concentration /M	E_{corr} /mV	i_{corr} / $\mu\text{A cm}^{-2}$	β_a /mV	β_c /mV	IE
–	20	0.1	–481	1380	141	–197	–
	30		–480	1513	169	–192	–
	40		–480	2818	164	–175	–
	60		–484	4600	195	–156	–
PVBT	20	1×10^{-5}	–440	537	75	–181	61.0
	30		–443	1096	100	–175	27.5
	40		–457	2089	128	–191	25.8
	60		–466	4808	93	–119	–4.5
	20	5×10^{-4}	–452	30	83	–127	97.8
	30		–450	37	117	–143	97.5
	40		–461	82	106	–153	97.0
	60		–462	211	90	–187	95.4
DPE	20	1×10^{-5}	–466	891	132	–166	35.4
	30		–445	1339	113	–156	11.5
	40		–449	2511	118	–138	10.9
	60		–472	4265	158	–182	7.2
	20	5×10^{-4}	–403	544	59	–223	60.5
	30		–409	660	72	–242	56.3
	40		–412	1241	85	–229	55.9
	60		–428	2691	102	–228	41.5
PVA	20	1×10^{-5}	–449	1196	114	–178	13.3
	30		–435	1412	102	–142	6.7
	40		–446	2691	122	–136	4.5
	60		–460	5011	94	–133	–8.9
	20	5×10^{-4}	–406	549	97	–292	60.2
	30		–405	851	103	–276	43.7
	40		–425	1659	113	–267	41.1
	60		–447	3981	131	–236	13.4
PVB	20	1×10^{-5}	–451	1071	114	–173	22.4
	30		–452	1348	111	–154	10.9
	40		–463	2570	133	–144	8.8
	60		–469	4285	160	–166	6.8
	20	5×10^{-4}	–408	660	88	–218	52.1
	30		–423	794	90	–222	47.5
	40		–425	1644	96	–218	41.6
	60		–443	3819	109	–201	16.9

where i_{inh} and i_{uninh} are the corrosion current densities for inhibited and uninhibited samples, respectively. The plot of θ vs. $\ln c$ shows that the adsorption obeys the Temkin adsorption isotherm (Equation 2).

$$e^{\theta} = K_{\text{ads}}c \quad (3)$$

where K is the adsorption equilibrium constant and f is the molecular interaction constant. The constant f depends on the intermolecular interaction in the adsorption layer and on the heterogeneity of the surface. If f is positive, mutual attraction of molecules occurs; if f is negative repulsion occurs [20].

A typical plot of θ vs. $\ln c$ for DPE both for polarisation and EIS data is shown in Figure 6. From the straight lines in the θ - $\log c$ graphs, equilibrium constants for the adsorption process, K_{ads} , were obtained. The equilibrium constants for are related to the free energy of adsorption, ΔG_{ads} , by,

$$K_{\text{ads}} = \frac{1}{55.5} \exp\left(\frac{-\Delta G_{\text{ads}}}{RT}\right) \quad (4)$$

where 55.5 is the molar concentration of water in the solution. The thermodynamic parameters for adsorption obtained from Temkin adsorption isotherms using surface coverage, θ , calculated from the results of both polarisation and EIS experiments are given in Table 3. The values of free energy of adsorption, ΔG_{ads} , are negative which reveals the spontaneity of the adsorption process and the stability of the adsorbed layer on the

steel surface. Since the value of ΔG_{ads} of -40 kJ mol^{-1} is usually accepted as a threshold value between chemisorption and physisorption, the obtained values of the adsorption free energy, ΔG_{ads} , are indicative of chemisorption [21–23]. Moreover the sign of the intermolecular interaction constants, f , is positive which indicates that the interaction between molecules causes the adsorption energy to increase with surface coverage.

Examination of polarisation data in Table 1 shows that the inhibition efficiency values follow the order PVBT > DPE > PVA > PVB. A similar order of inhibition efficiency obtained from EIS was observed from examination of the Nyquist diagram for carbon steel in 0.1 M HCl solution with 1×10^{-4} M PVBT, DPE, PVA and PVB shown in Figure 7. The effectiveness of a compound as an inhibitor depends on its structure. The variation in efficiency mainly depends on the type and the nature of the substituents in the inhibitor molecule. The difference in protection actions can be attributed to the presence of substituents that increase or decrease the electron density on the azomethine ($-\text{C}=\text{N}-$) group. The difference in inhibition efficiency between PVBT and DPE arises from the presence of thiophenol in PVBT instead of the presence of a π electron deficient ring (i.e. pyridine) as a substituent in DPE. Thiophenol increases the electron density on the azomethine group and the $-\text{SH}$ group acts as an additional adsorption centre.

In the PVA molecule the following tautomeric equilibrium may take place:

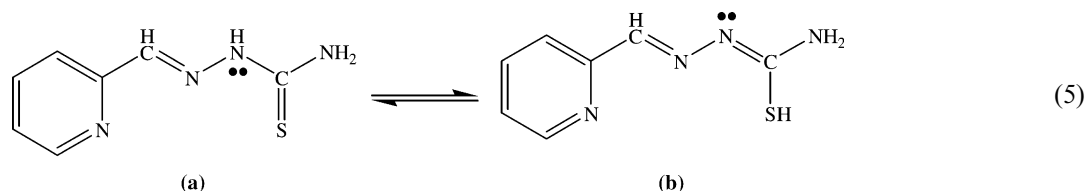


Table 3. Thermodynamic parameters of adsorption obtained by Tafel polarisation and AC impedance measurements for studied Schiff bases on carbon steel in 0.1 M HCl solutions at 20 °C

Inhibitor	Equilibrium constant of adsorption $K_{\text{ads}} (\times 10^5)$		Standard free energy of adsorption $\Delta G_{\text{ads}} / \text{kJ mol}^{-1}$		Molecular interaction constant f	
	$(K_{\text{ads}})_p$	$(K_{\text{ads}})_z$	$(\Delta G_{\text{ads}})_p$	$(\Delta G_{\text{ads}})_z$	f_p	f_z
PVBT	75.9	8.63	-48.38	-43.08	7.64	10.99
DPE	20.2	4.65	-45.15	-41.73	11.34	11.34
PVA	3.40	3.56	-40.81	-40.92	8.68	10.55
PVB	7.30	4.20	-42.67	-41.33	11.92	17.24

* $(K_{\text{ads}})_p$, $(\Delta G_{\text{ads}})_p$, f_p Tafel polarisation results, $(K_{\text{ads}})_z$, $(\Delta G_{\text{ads}})_z$, f_z AC impedance results.

Table 4. Calculated dihedral angle values of studied Schiff bases

Inhibitor	α	β	γ
PVBT	1.266	0.448	91.618
DPE	12.497	6.814	50.672
PVA	-1.142	-0.775	102.053
PVB	0.000	-180.000	179.553

Calculated dihedral angles of atoms numbered as: $\alpha = 4,5,7,9$; $\beta = 5,7,9,10, 12$; $\gamma = 7,9,10,11$.

Table 5. Activation parameters of dissolution reaction of low carbon steel in 0.1 M HCl solution containing 1×10^{-5} and 5×10^{-4} M concentrations of studied Schiff bases

Inhibitor	Concentration /M	E_a /kJ mol ⁻¹	ΔH^* /kJ mol ⁻¹	ΔS^* /kJ mol ⁻¹
–	0.1	26.28	23.68	-0.105
PVBT	1×10^{-5}	41.52	38.95	-0.085
	5×10^{-4}	44.16	41.49	-0.050
DPE	1×10^{-5}	32.37	29.93	-0.086
	5×10^{-4}	33.91	31.31	-0.086
PVA	1×10^{-5}	30.79	28.15	-0.091
	5×10^{-4}	40.92	38.45	-0.061
PVB	1×10^{-5}	29.58	24.92	-95.30
	5×10^{-4}	37.36	34.69	-73.49

therefore a certain fraction of the PVA may exist in the mercapto tautomeric form b. When PVA exists in b form, the electron withdrawing effect of the $-C=N-$ double bond decreases the electron density on the imine group. Thus lower inhibition efficiency of PVA compared to DPE can be explained by the existence of a certain fraction of PVA in the b form. The inhibition efficiency of PVB is lower than PVA. This can be explained by the planar structure of PVB (Figure 1). In order to clarify the planarity of PVB, the values of dihedral angles were calculated by energy minimisation using Chem3-D program (CS Chem Office) [24]. Values of dihedral angles (Table 4) show that PVB exists in transoid structure and due to this structure full conjugation becomes feasible in PVB which decreases the electron density on the imine group.

The fact that the inhibition efficiencies decreased with increase in temperature suggests weakening of physical adsorption of the Schiff bases. Physical adsorption in the inhibition of corrosion of carbon steel in acidic solution is small but important because it is the preceding stage of chemisorption.

In order to calculate activation parameters for the corrosion process the Arrhenius (Equation 5) and the transition state equations (Equation 6) were used.

$$k = A \exp[E_a/RT] \quad (6)$$

$$k = \frac{RT}{Nh} \exp(\Delta S^*/R) \exp(-\Delta H^*/RT) \quad (7)$$

Kinetic parameters obtained from plots of $\ln i_{\text{corr}}$ vs. $1/T$ and $\ln (i_{\text{corr}}/T)$ vs. $1/T$ graphs for the studied Schiff bases are given in Table 5. Inspection of Table 5 shows that higher values were obtained for E_a and ΔH^* in the presence of inhibitors indicating the higher protection efficiency observed for these inhibitors. There is also a parallelism between increases in inhibition efficiency and increases in E_a and ΔH^* values. On the other hand ΔS^* values were found to be negative in acid solution in the absence of inhibitor whereas ΔS^* values were positive in the presence of the inhibitors. Adsorption of inhibitor molecules hinders H_2 evolution, so the entropy of activation is more positive in the presence of inhibitor.

4. Conclusions

A systematic study of corrosion inhibition of low carbon steel in 0.1 M HCl by four Schiff bases has led to the following main conclusions:

- All the Schiff bases are found to perform well as corrosion inhibitors in 0.1 M HCl solution for low carbon steel and the inhibition efficiency values follow the order PVBT > DPE > PVA > PVB. The inhibition efficiencies were found to be depend on the type and the nature of the substituent present in the inhibitor molecule.
- The inhibition efficiencies increase with increasing inhibitor concentration and with decreasing temperature.
- Activation parameters (E_a , ΔH^* , ΔS^*) for the corrosion of low carbon steel in HCl were calculated and indicate that corrosion is much reduced in the presence of inhibitors.
- Tafel behaviour indicates that corrosion inhibition of low carbon steel in 0.1 M HCl by the Schiff bases is under the anodic control.
- The increase in charge transfer resistance, R_t , values of inhibitor with increase in Schiff base concentrations shows that inhibition abilities of the Schiff bases depend on the degree of adsorption of the molecule on the metal surface.
- Adsorption on low carbon steel in 0.1 M HCl solution was found to obey the Temkin adsorption isotherm.

References

1. M.N. Desai, M.B. Desai, C.B. Shah and S.M. Desai, *Corros. Sci.* **26** (1986) 827.
2. G.K. Gomma and M.H. Wahdan, *Mater. Chem. Phys.* **39** (1995) 209.
3. S.L. Li, S. Chen, S.B. Lei, H. Ma, R. Yu and D. Liu, *Corros. Sci.* **41** (1999) 1273.
4. A. Raman and P. Labine, 'Reviews on Corrosion Inhibitor Science and Technology' (NACE, Houston, 1986), p. 20.
5. H. Shorkey, M. Yuasa, I. Sekine, R.M. Issa, H.Y. El-Baradie and G.K. Gomma, *Corros. Sci.* **40** (1998) 2173.
6. C.D. Bain, E.B. Throughton, Y.T. Tao, J. Evall, G.M. Whiteside and J.G. Nuzzo, *J. Am. Soc.* **111** (1989) 321.
7. R.G. Nuzzo, E.M. Korenic and L.H. Dubois, *J. Chem. Phys.* **93** (1990) 767.

8. Z. Quan, S.H. Chen, Y. Li and X. Cui, *Corros. Sci.* **44** (2002) 703.
9. S.L. Li, Y.G. Wang, S.H. Chen, R. Yu, S.B. Lei, H.Y. Ma and D.X. Liu, *Corros. Sci.* **41** (1999) 1769.
10. B. Erk, A. Dilmac, Y. Baran and A. Balaban, *Synth. React. Inorg. Met. Org. Chem.* **10** (2000) 30.
11. N.I. Dodoff, Ü. Özdemir, N. Karacan, M.C. Georgieva, S.M. Konstantinov and M.E. Stefanova, *Z. Naturforsch* **54 B** (1999) 1553.
12. F.E. Anderson, C.J. Duca and J.V. Scudi, *J. Am. Chem. Soc.* **73** (1951) 4967.
13. N.K. Jha and D.M. Joshi, *Synth. React. Inorg. Met. Org. Chem.* **14** (1984) 455.
14. T. Vasudevan, B. Muralidharan, S. Muralidharan and S. Venkatakrishna Iyer, *Anti-Corros. Method M.* **45** (1998) 120.
15. F. Mansfeld, M.W. Kending and W.J. Lorenz, *J. Electrochem. Soc.* **132** (1985) 290.
16. F. Mansfeld, *Corrosion* **37** (1981) 301.
17. E. McCaferty, *Corros. Sci.* **39** (1997) 243.
18. Z. Quan, X. Wu, S. Chen, S. Zhao and H. Ma, *Corrosion* **57** (2001) 195.
19. F. Mansfeld, 'Corrosion Mechanisms' (Marcel Dekker, New York, 1987), pp. pp. 119.
20. Z. Szlarska-Smialowska. Proceedings of Advanced Study Institute on Electrochemical and Optical Techniques for the Study and Monitoring of Metallic Corrosion, in M.G.S. Ferreira and Melenderes C.A. (Eds.), NATO ASI Series E: Applied Sciences Vol.203, (Kluwer Academic Publishers, Netherlands, 1991), pp. 285.
21. P.W. Atkins, 'Physical Chemistry', 6th edition (Oxford University Press, 1999), 857 pp.
22. M. Hosseini, S.F.L. Mertens, M. Ghorbani and M.R. Arshadi, *Mater. Chem. Phys.* **78** (2003) 800.
23. Z. Szlarska-Smialowska, *Corros. Sci.* **18** (1978) 953.
24. CS Chem Office, Cambridge Scientific and Computing Inc., Suite 61, 875 Massachusetts Avenue, Cambridge, MA 02139, USA.